



**UNIVERSITI PUTRA MALAYSIA**

**STUDIES OF THE PROPERTIES OF SPUTTERED CoAg AND CoNiAg  
GRANULAR MAGNETIC THIN FILMS**

**HUDA ABDULLAH**

**FSAS 2002 49**

**STUDIES OF THE PROPERTIES OF SPUTTERED CoAg AND CoNiAg  
GRANULAR MAGNETIC THIN FILMS**

**By**

**HUDA ABDULLAH**

**Thesis Submitted to the School of Graduate Studies, Universiti Putra Malaysia,  
in Fulfilment of the Requirement for the Degree of Master of Science**

**May 2002**



***DEDICATION***

***Special dedication to:***

**My beloved family**

**Abstract of thesis presented to the Senate of Universiti Putra Malaysia in fulfilment  
of the requirements for the degree of Master of Science**

**STUDIES OF THE PROPERTIES OF SPUTTERED CoAg AND CoNiAg  
GRANULAR MAGNETIC THIN FILMS**

**By**

**HUDA ABDULLAH**

**May 2002**

**Chairman: Professor Abdul Halim Shaari, Ph.D.**

**Faculty: Science and Environmental Studies**

The observation of the magnetoresistance effect has been focussed on the studies of the giant magnetoresistance (GMR) effect, throughout the world, by researchers and scientists after its discovery from magnetic multilayer. It has later been observed in granular alloys in which nanometer-sized magnetic granules such as Co, Ni, Fe, are embedded in an immiscible metallic matrix (Ag, Cu, Au, etc.). These magnetic alloys having GMR effect find potential applications in magnetic field sensor and read heads.

In this work, granular thin films of CoAg and CoNiAg alloys have been prepared using Radio frequency (RF) Magnetron sputtering technique. A split target composed of high purity (99.99%) Co, Ni and Ag metals have been bombarded with argon atoms to form plasma, which condensed onto the glass substrate to form thin films of various thicknesses depending on the deposition time and RF power. The

characteristics and magnetotransport properties of GMR materials based on the CoAg and CoNiAg have been investigated. Magnetoresistance (MR) is usually expressed as the fractional change in resistance of a specimen produced by an applied field,  $GMR = \Delta R/R$ . For non-magnetic films MR is quite small, however the presence of magnetic entities in the non-magnetic matrix, increases its MR and hence it is termed as GMR.

The surface morphology and the structure of the films had been examined using a scanning electron microscope (SEM). It has been observed that the surface morphology was smooth and homogeneous with little contamination on the films surfaces, due to oil spots and time debris throughout the deposition process and sample preparation for various measurements. The composition and the element percentage for each series were determined through EDX microanalyser installed in the SEM unit. The optimum percentage for this ferromagnetic element of Co is about 23.32%. At this composition of Co, sample has the highest value of MR. The structures of samples were analyzed by using PHILIPS X-ray diffractometer. The X-ray diffraction indicates a uniform fcc structure and set of  $<111>$ ,  $<200>$ ,  $<220>$  and  $<311>$  peaks were observed. The  $<111>$  peak shows higher intensity indicated that the growth of  $<111>$  Ag structure is dominant. It was observed that  $<111>$  peaks are broad and hence could be deduced that these granular films are well distributed with small grain size. As the peak of  $<111>$  is broad, the value of MR is increase.

The MR effect had been measured using a standard four-point probe technique and the measurements extended from room temperature to 100 K by using liquid nitrogen cryostat. The increase of maximum MR for as-deposited samples

from 1.83% at room temperature to 2.83% at 100 K were observed in  $\text{Co}_{23.32}\text{Ag}_{76.68}$  ( $\text{Co5Ag}$  (d.t. $50^\circ\text{C}$ )) film deposited for 70 minutes. The value of MR depends on the density and the size distribution of ferromagnetic entities. The results also show that the GMR values have not achieved saturation condition at an applied field of 1 Tesla at any temperature. This could be due to the small clusters in the film that need higher external field to totally align the magnetic moment along the field axis. This is also supported by the broadening of XRD peaks.

The highest MR for the annealed sample of  $\text{Co}_{29.63}\text{Ag}_{70.37}$  ( $\text{Co6Ag}$  (d.t. $50^\circ\text{C}$ )) deposited for 80 minutes is approximately to 2.95%. This sample is almost saturated at 1 Tesla when the sample was annealed at  $350^\circ\text{C}$  for 30 minutes. The increase in the GMR values following the heat treatment is believed to be mainly due to particle growth that depends on both the size and the density of magnetic grains.

Abstrak tesis yang kemukakan kepada Senat Universiti Putra Malaysia sebagai  
memenuhi keperluan untuk Ijazah Master Sains

**KAJIAN CIRI-CIRI KEMAGNETORINTANGAN BAGI FILEM-FILEM  
NIPIS CoAg DAN CoNiAg**

**Oleh**

**HUDA BINTI ABDULLAH**

**Mei 2002**

**Pengerusi: Profesor Abdul Halim Shaari, Ph.D.**

**Fakulti: Sains dan Pengajian Alam Sekitar**

Pemerhatian kesan magnetorintangan adalah lebih menarik telah difokuskan dalam satu kajian tentang kesan magnetorintangan gergasi (MRG) di seluruh dunia, dengan penyelidikan-penyeleidikan dan ahli-ahli sains setelah ianya dijumpai daripada berbilang lapisan magnetik. Kemudian, ianya telah diperhatikan dalam berpepasir aloi-aloi di mana butiran magnetik bersaiz nanometer seperti Co, Ni, Fe, adalah terbenam dalam matriks metalik tak tercampurkan (Ag, Cu, Au, sbg.). Aloialoi magnetik ini yang mempunyai kesan MRG menjumpai keupayaan aplikasi dalam pengesan medan magnet dan *read head*.

Dalam penyelidikan ini, butiran saput tipis daripada aloi-aloi CoAg dan CoNiAg telah disediakan dalam teknik percikan RF Magnetron. Sasaran pisahan mempunyai ketulenan tinggi (99.99%) logam Co dan Ag telah ditembak secara bertalu-talu dengan atom-atom argon kepada bentuk plasma, di mana akan berubah menjadi cecair ke atas substrak kaca kepada bentuk filem nipis dengan pelbagai

ketebalan yang bergantung kepada masa pemendapan dan kuasa R.F. Ciri-ciri dan sifat-sifat magnetoangkutan daripada bahan-bahan magnetorintangan gergasi berdasarkan kepada CoAg telah diselidiki. magnetorintangan (MR) biasanya dinyatakan sebagai perubahan berperingkat suatu specimen kerintangan dihasilkan oleh medan yang dikenakan,  $MRG = \Delta R/R$ . Untuk filem bukan magnetik nilai MR adalah terlalu kecil, walau bagaimanapun, dengan kewujudan entiti magnetik dalam matrik bukan magnetic akan meningkatkan MR, sebagai takrifan bagi MRG.

Morfologi dan struktur permukaan bagi filem-filem telah diperiksa menggunakan mikroskop electron pengimbasan (SEM). Ia telah diperhatikan bahawa morfologi permukaan adalah licin dan homogen, dan terdapat sedikit sahaja kontaminasi pada permukaan-permukaan filem ini. Ia boleh disebabkan oleh bintik-bintik minyak dan kesan tapak jari seluruh proses pemendapan dan penyediaan sampel untuk pelbagai pengukuran. Komposisi dan peratusan unsure-unsur untuk setiap siri telah ditentukan menggunakan penganalisis penyebaran tenaga sinaran-X (EDX) tersedia dalam unit SEM. Peratusan optima untuk unsur ferromagnetic ini, Co adalah kira-kira 23.32%. Pada komposisi cobalt ini, sample mempunyai nilai MR yang paling tinggi. Walau bagaimanapun, struktur sampel dianalisis dengan menggunakan Pembelauan sinar-X PHILIPS. Pembelauan sinar-X menunjukkan satu bentuk struktur fcc dengan nyata komposisi bergantung kepada parameter kekisi. Spektra XRD menunjukkan set puncak-puncak  $<111>$ ,  $<200>$ ,  $<220>$  dan  $<311>$  telah diperhatikan. Puncak  $<111>$  Ag menunjukkan keamatan yang tinggi yang menunjukkan struktur  $<111>$  Ag yang dominan. Ia telah diperhatikan bahawa puncak  $<111>$  Ag adalah lebar dan boleh disimpulkan bahawa granular filem-filem

ini bertaburan rapi dengan saiz butiran kecil. Puncak <111> Ag melebar, maka nilai MR akan meningkat.

Kesan magnetorintangan telah diukur dengan menggunakan teknik penduga empat-panggal piawai dan pengukuran dilakukan dari suhu bilik hingga ke 100 K dengan menggunakan cecair nitrogen cryostat. Peningkatan maksimum MR untuk sampel disimpan dari 1.83% pada suhu bilik ke 2.83% pada 100 K diperoleh dari  $\text{Co}_{23.32}\text{Ag}_{76.68}$  (suhu pemendapan  $50^\circ\text{C}$ ) dimendap selama 70 minit. Nilai MR bergantung kepada ketumpatan dan taburan saiz entiti ferromagnetic. Lengkungan-lengkungan MRG juga menunjukkan bahawa nilai MRG tidak mencapai keadaan ketepuan ketika medan yang dikenakan 1 Tesla pada mana-mana suhu. Ini boleh disebabkan oleh kelompok-kelompok kecil dalam filem yang memerlukan medan luaran yang tinggi untuk menjajarkan momen magnetic sepanjang paksi medan. Ini juga telah disokong oleh kelebaran puncak XRD.

Nilai tertinggi MR untuk sampel sepuh lindap diperolehi oleh  $\text{Co}_{29.63}\text{Ag}_{70.37}$  (suhu pemendapan  $50^\circ\text{C}$ ) dimendap selama 80 minit adalah menghampiri 2.95%. Sampel ini hampir tepu pada 1 tesla apabila sample disepuh-lindapkan pada  $350^\circ\text{C}$  selama 30 minit. Peningkatan nilai MRG berikut dengan rawatan pemanasan yang dipercayai menjadi punca utama yang menyebabkan pertumbuhan zarah-zarah yang bergantung kepada kedua-dua saiz dan ketumpatan butiran-butiran magnetik.

## **ACKNOWLEDGEMENTS**

First and foremost, I would like to acknowledge my supervisor, Professor Dr. Abdul Halim Shaari, for giving me the platform to pursue my studies and gave me the opportunity to explore the Giant Magnetoresistance (GMR) of granular magnetic material and its application, besides the constant support throughout this work.

It is pleasure to acknowledge my co-supervisor Associate Professor Dr. W. Mahmood Mat Yunus and Associate Professor Dr. Elias Saion for his commands suggestion throughout this project.

Special thanks to my working colleagues, Lim Kim Pah and Kabashi khatir kabashi for their helpful discussions and suggestions on this work, and also for their helping on the operating all the equipment in the laboratory. And further my thankful also to Imad, Ari Sulistrorini, and Iftetan and not forgotten to Som.

Particular thanks are also owed to En. Razak for his help in setting up the four-point probe resistance measurement system, the XRD machine, annealing furnace and other technical help needed in this work.

I would like to extend my appreciation to En. Yusof in Physics Department, University Malaya and also En. Ismail in Mechanical department, University Malaya for their helping on SEM and EDX measurement.

The financial support in this work from the Ministry of Science and technology, under the IRPA vote: 09-02-04-0019 (Giant magnetoresistive and Magneto resistive Material) is also gratefully acknowledged. Without this support, it is possible for us to pursue this project with success. Lastly, I would like to extend my gratitude to the government for granting the National Science Fellowship (NSF) Scholarship to me for supporting my daily expenditure.

I certify that an Examination Committee met on 20<sup>th</sup> May 2002 to conduct the final examination of Huda Abdullah on her Master of Science thesis entitled "Studies the Properties of Sputtered CoAg and CoNiAg Granular Magnetic Thin Films" in accordance with Universiti Pertanian Malaysia (Higher Degree) Act 1980 and Universiti Pertanian Malaysia (higher Degree) Regulations 1981. The Committee recommends that the candidate be awarded the relevant degree. Members of the Examination Committee are as follows:

**ZAIDAN ABD. WA AB, Ph.D.**  
Faculty of Science and Environmental Studies,  
Universiti Putra Malaysia  
(Chairman)

**ABDUL ALIM S AA I, Ph.D.**  
Professor  
Faculty of Science and Environmental Studies,  
Universiti Putra Malaysia  
(Member)

**W. MAHMOOD MAT YUNUS, Ph.D.**  
Associate Professor  
Faculty of Science and Environmental Studies,  
Universiti Putra Malaysia  
(Member)

**ELIAS BIN SAION, Ph.D.**  
Associate Professor  
Faculty of Science and Environmental Studies,  
Universiti Putra Malaysia  
(Member)

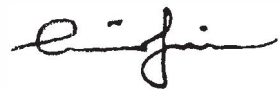


---

**SHAMSHER MO AMAD AMADILI, Ph.D.**  
Professor/Deputy Dean  
School of Graduate Studies  
Universiti Putra Malaysia

Date : 21 JUN 2002

This thesis submitted to the Senate of Universiti Putra Malaysia has been accepted  
as fulfilment of the requirement for the degree of Master of Science.



---

**AINI IDERIS, Ph.D.**  
Professor/Dean,  
School of Graduate Studies,  
Universiti Putra Malaysia

Date: 08 AUG 2002

I hereby declare that the thesis is based on my original work except for quotations and citations, which have been duly acknowledged. I also declare that it has not been previously or concurrently submitted for any other degree at UPM or other institutions.

  
HUDA BINTI ABDULLAH  
Date: 21/6/2022

## TABLE OF CONTENT

	<b>Page</b>
<b>DEDICATION</b>	ii
<b>ABSTRACT</b>	iii
<b>ABSTRAK</b>	vi
<b>ACKNOWLEDGEMENTS</b>	ix
<b>APPROVAL SHEETS</b>	xi
<b>DECLARATION FORM</b>	xiii
<b>LIST OF TABLES</b>	xvi
<b>LIST OF FIGURES</b>	xvii
<b>LIST OF ABBREVIATIONS AND GLOSSARY OF TERMS</b>	xxii
 <b>CHAPTER</b>	
<b>I           INTRODUCTION</b>	
1.1 What is Giant Magnetoresistance (GMR)?	1
1.1.1 GMR in Multilayer Thin Film	2
1.1.2 GMR in Granular Thin Film	3
1.2 Application of Giant Magnetoresistance	3
1.3 Objective	6
<b>II          LITERATURE REVIEW</b>	
2.1 Theory of Spin-dependent Conductivity in GMR Materials	7
2.2 Classification of Magnetoresistance	11
2.3 Giant Magnetoresistance of Granular Thin Film	13
2.4 Model Calculation	16
2.5 Microstructure	21
2.6 Giant Magnetoresistance Effects	23
2.6.1 Thickness-Dependence	24
2.6.2 Composition-Dependence	26
2.6.3 Thermal-Dependence	29
<b>III        THEORY</b>	
3.1 Ferromagnetism	36
3.1.1 Magnetization of Ferromagnetic Thin Layers	36
3.1.2 Magnetic Domains	37
3.1.3 Magnetic Anisotropy	38
3.2 Thin Films	39
3.2.1 Theory of Thin Film	39
3.2.2 Thin Film Growth Process	39
3.2.3 Thin Film Deposition Process	40
3.2.3.1 Vacuum Deposition	40
3.2.3.2 Laser Deposition	41
3.2.3.3 Molecular Beam Epitaxy (MBE)	41
3.2.3.4 Ion Plating Deposition	42
3.2.3.5 Activated Reactive Evaporation (ARE)	43
3.2.3.6 Ionized Cluster Beam Deposition (ICBD),	44

	3.2.3.7 Chemical Vapour Deposition (CVD)	45
	3.2.4 Deposition Condition	45
3.3	Sputtering Phenomenon	46
	3.3.1 Sputter Yield	47
	3.3.2 Velocity and Mean Free Path	48
	3.3.3 Mechanism Sputtering	49
	3.3.4 Sputtering System	50
	3.3.4.1 Glow Discharge	50
	3.3.4.2 DC Sputtering	52
	3.3.4.3 RF Sputtering	53
	3.3.4.4 Magnetron Sputtering	55
<b>IV</b>	<b>METHODOLOGY AND SAMPLE PREPARATION</b>	
4.1	Preparation of Samples	57
	4.1.1 RF Magnetron Sputtering Technique	58
	4.1.2 Annealing Process	60
4.2	Characterization of Samples	61
	4.2.1 Magnetoresistance(MR) Measurement	61
	4.2.2 Electron Diffractor X-Ray (EDX) Analysis	63
	4.2.3 Scanning Electron Microscope (SEM)	63
	4.2.4 Estimation of thickness	64
	4.2.5 X-Ray Diffraction (XRD) Measurement	65
4.3	Errors of Measurements	69
<b>V</b>	<b>RESULTS AND DISCUSSION</b>	
5.1	Scanning Electron Microscope (SEM) Images	70
5.2	Energy Dispersive X-ray (EDAX) Analysis	75
5.3	X-Ray Diffraction (XRD) Analysis	82
5.4	Magnetoresistance (MR) Measurements	89
5.5	Annealing Effect	105
<b>VI</b>	<b>CONCLUSION AND SUGGESTIONS</b>	
	Conclusion	129
	Suggestion for Further Research	131
	<b>REFERENCES</b>	133
	<b>APPENDIX</b>	
A	A.1 – A.2: MR values for as-deposited and annealed samples	142
	A.3 – A.8: Graphs of the MR measurement for as-deposited samples	144
B	The effect of deposition rate on MR for samples annealed at 350°C and 400°C for 30 minutes	160
C	Tables of formulas for calculation of Interplanar spacing, $d_{hkl}$	162
	<b>BIODATA</b>	164

## LIST OF TABLES

<b>Table</b>		<b>Page</b>
1	Deposition conditions and the crystalline properties	46
2	Estimation of the thickness	64
3	Estimated errors of measurement	69
4	The boulders size in each SEM images	74
5	The percentage obtained by EDX with the surface area of each composition	81
6	The Ag (111) phase positions and d spacing for each composition	86

## LIST OF FIGURES

<b>Figure</b>		<b>Page</b>
1	Giant magnetoresistance in term of spin-dependent electron scattering (top diagrams) and represented by an equivalent resistance circuit (bottom diagrams).	9
2	GMR nanostructure and their magnetoresistance behaviour for granular thin film.	14
3	Thin film deposition processes	40
4	Molecular Beam Epitaxy (MBE) System	42
5	Ion Plating	43
6	Activated Reactive Evaporative (ARE)	44
7	Schematic of dc sputtering system	47
8	Incident ions and the sputtered particles	49
9	Cycloidal motion of electrons in a magnetic field	51
10	Electron trajectory in a crossed electromagnetic field.	52
11	RF-diode sputtering system	54
12	Impedance matching networks for RF-sputtering system	55
13	Planar Magnetron Sputtering System	56
14	Composite target for deposition film	57
15	The Edwards ESM100 sputtering system	58
16	The Construction for four-point probe	61
17	The Basic system used to measure the MR value of thin film	62
18	SEM samples preparations	64
19	Geometry of the Bragg reflection analogy.	66

20	PHILIPS X-Ray Diffractometer beam path.	68
21 (a)	SEM image of the Co <sub>4</sub> Ag (d.t.50°C)	70
21 (b)	SEM image of the Co <sub>5</sub> Ag (d.t.50°C)	71
21 (c)	SEM image of the Co <sub>6</sub> Ag (d.t.50°C)	71
21 (d)	SEM image of the Co <sub>7</sub> Ag (d.t.50°C)	72
21 (e)	SEM image of the Co <sub>5</sub> Ag (d.t.100°C)	72
21 (f)	SEM image of the Co <sub>6</sub> Ag (d.t.100°C)	73
22 (a)	EDX pattern for samples Co <sub>3</sub> Ag (d.t.50°C)	75
22 (b)	EDX pattern for samples Co <sub>4</sub> Ag (d.t.50°C)	76
22 (c)	EDX pattern for samples Co <sub>5</sub> Ag (d.t.50°C)	76
22 (d)	EDX pattern for samples Co <sub>6</sub> Ag (d.t.50°C)	77
22 (e)	EDX pattern for samples Co <sub>7</sub> Ag (d.t.50°C)	77
22 (f)	EDX pattern for samples Co <sub>8</sub> Ag (d.t.50°C)	78
22 (g)	EDX pattern for samples Co <sub>9</sub> Ag (d.t.50°C)	78
22 (h)	EDX pattern for samples Co <sub>5</sub> Ag (d.t.100°C)	79
22 (i)	EDX pattern for samples Co <sub>6</sub> Ag (d.t.100°C)	79
22 (j)	EDX pattern for samples Co <sub>5</sub> Ni <sub>2</sub> Ag (d.t.100°C)	80
22 (k)	EDX pattern for samples Co <sub>5</sub> Ni <sub>3</sub> Ag (d.t.100°C)	80
23 (a)	The XRD pattern for Co <sub>5</sub> Ag (d.t.50°C)	82
23 (b)	The XRD pattern for Co <sub>6</sub> Ag (d.t.50°C)	83
23 (c)	The XRD pattern for Co <sub>5</sub> Ag (d.t.100°C)	83
23 (d)	The XRD pattern for Co <sub>6</sub> Ag (d.t.100°C)	84
23 (e)	The XRD pattern for Co <sub>5</sub> Ni <sub>3</sub> Ag (d.t.100°C)	84
23 (f)	The XRD pattern for Co <sub>5</sub> Ni <sub>2</sub> Ag (d.t.100°C)	85
24	X-Ray Diffraction patterns for the as-deposited Co <sub>x</sub> Ag <sub>100-x</sub> (d.t.50°C) samples as a function of Co concentration.	87

25 (a)	Magnetic field dependence of MR for Co <sub>4</sub> Ag (d.t. 50°C) samples measured at room temperature	90
25 (b)	Magnetic field dependence of MR for Co <sub>5</sub> Ag (d.t. 50°C) samples measured at room temperature	91
25 (c)	Magnetic field dependence of MR for Co <sub>6</sub> Ag (d.t. 50°C) samples measured at room temperature	91
25 (d)	Magnetic field dependence of MR for Co <sub>5</sub> Ag (d.t. 100°C) samples measured at room temperature	92
25 (e)	Magnetic field dependence of MR for Co <sub>6</sub> Ag (d.t. 100°C) samples measured at room temperature	92
25 (f)	Magnetic field dependence of MR for Co <sub>5</sub> Ni <sub>3</sub> Ag (d.t. 100°C) samples measured at room temperature	93
25 (g)	Magnetic field dependence of MR for Co <sub>5</sub> Ni <sub>2</sub> Ag (d.t. 100°C) samples measured at room temperature	93
26	Temperature dependence of GMR at 1 Tesla of sample deposited for 70 minutes of each composition	96
27	The Variation of GMR values of the CoAg and CoNiAg thin films with the deposition rates (thickness) of the film	98
28	The Variation of GMR values with the percentage of cobalt element in the thin film	99
29	The Variation of GMR values with the percentage of silver element in the thin film	100
30 (a)	The linear relation between square of % GMR and applied field, H for Co <sub>4</sub> Ag (d.t.50°C) samples	101
30 (b)	The linear relation between square of % GMR and applied field, H for Co <sub>5</sub> Ag (d.t.50°C) samples	101
30 (c)	The linear relation between square of % GMR and applied field, H for Co <sub>6</sub> Ag (d.t.50°C) samples	102
30 (d)	The linear relation between square of % GMR and applied field, H for Co <sub>5</sub> Ag (d.t.100°C) samples	102
30 (e)	The linear relation between square of % GMR and applied field, H for Co <sub>6</sub> Ag (d.t.100°C) samples	103
30 (f)	The linear relation between square of % GMR and applied field, H for Co <sub>5</sub> Ni <sub>2</sub> Ag (d.t.100°C) samples	103

30 (g)	The linear relation between square of % GMR and applied field, H for Co5Ni3Ag (d.t.100°C) samples	104
31 (a)	The magnetic field dependence of the MR for Co4Ag (d.t.50°C) annealed samples at $T_a = 350^\circ\text{C}$ for 30 minutes	105
31 (b)	The magnetic field dependence of the MR for Co4Ag (d.t.50°C) annealed samples at $T_a = 400^\circ\text{C}$ for 30 minutes.	106
31 (c)	The magnetic field dependence of the MR for Co5Ag (d.t.50°C) annealed samples at $T_a = 400^\circ\text{C}$ for 30 minutes.	106
31 (d)	The magnetic field dependence of the MR for Co5Ag (d.t.50°C) annealed samples at $T_a = 350^\circ\text{C}$ for 30 minutes.	107
31 (e)	The magnetic field dependence of the MR for Co6Ag (d.t.50°)	107
31 (f)	The magnetic field dependence of the MR for Co5Ag (d.t.100°C) annealed samples at $T_a = 350^\circ\text{C}$ for 30 minutes.	108
31 (g)	The magnetic field dependence of the MR for Co5Ni2Ag (d.t.100°C) annealed samples at $T_a = 350^\circ\text{C}$ for 30 minutes.	108
31 (h)	The magnetic field dependence of the MR for Co5Ni3Ag (d.t.100°C) annealed samples at $T_a = 350^\circ\text{C}$ for 30 minutes.	109
32 (a)	The annealed sample of Co5Ag (d.t.50°C) deposited for 60 minutes	111
32 (b)	The XRD pattern for annealed sample of Co5Ag (d.t.50°C) deposited for 60 minutes	112
32 (c)	The annealed sample of Co5Ag (d.t.50°C) deposited for 80 minutes	113
32 (d)	XRD pattern for annealed sample of Co5Ag (d.t.50°C) deposited for 80 minutes	114
33 (a)	The annealed sample of Co4Ag (d.t.50°C) deposited for 60 minutes	115
33 (b)	The XRD pattern for annealed sample of Co4Ag (d.t.50°C) deposited for 60 minutes	115
34 (a)	The annealed sample of Co6Ag (d.t.50°C) deposited for 80 minutes	116
34 (b)	The XRD pattern for annealed sample of Co6Ag (d.t.50°C) deposited for 80 minutes	117

34 (c)	The annealed sample of Co <sub>6</sub> Ag (d.t.50°C) deposited for 60 minutes	118
34 (d)	The XRD pattern for annealed sample of Co <sub>6</sub> Ag (d.t.50°C) deposited for 60 minutes	118
35 (a)	The annealed sample of Co <sub>5</sub> Ag (d.t.100°C) deposited for 80 minutes	119
35 (b)	The XRD pattern for annealed sample of Co <sub>5</sub> Ag (d.t.100°C) deposited for 80 minutes	120
36 (a)	The annealed sample of Co <sub>5</sub> Ni <sub>2</sub> Ag (d.t.100°C) deposited for 80 minutes	120
36 (b)	XRD pattern for annealed sample of Co <sub>5</sub> Ni <sub>2</sub> Ag (d.t.100°C) deposited for 80 minutes	121
37 (a)	The annealed sample of Co <sub>5</sub> Ni <sub>3</sub> Ag (d.t.100°C) deposited for 70 minutes	122
37 (b)	The annealed sample of Co <sub>5</sub> Ni <sub>3</sub> Ag (d.t.100°C) deposited for 60 minutes	122
37 (c)	The annealed sample of Co <sub>5</sub> Ni <sub>3</sub> Ag (d.t.100°C) deposited for 60 minutes	123
37 (d)	XRD pattern for annealed sample of Co <sub>5</sub> Ni <sub>3</sub> Ag (d.t.100°C) deposited for 60 minutes	124
38	Magnetic field dependence of the MR for the best-annealed samples of the four series	125
39	The XRD diffraction pattern of the best annealed samples of the four series	127

## LIST OF ABBREVIATIONS AND GLOSSARY OF TERMS

Abbrev/Gloss	Description
$\alpha, \beta, \gamma$	Phase designations
$\theta$	Bragg diffraction angle
$^{\circ}\text{C}$	Degree Celsius
$\rho_{\uparrow}$	Spin-up resistivity
$\rho_{\downarrow}$	Spin-down resistivity
$\rho_F$	Ferromagnetic resistivity
$\rho_N$	Non Ferromagnetic resistivity
$\rho_{\parallel}$	Parallel resistivity
$\rho_{\perp}$	Transverse resistivity
$\rho_{\perp}$	Perpendicular resistivity
$\rho_0$	Resistivity due to impurity
$\rho_H$	Resistivity at applied magnetic field H
$\rho_{\text{ave}}$	Average resistivity
$\rho_m$	Magnetic resistivity
$\Delta\rho_{\text{AMR}}$	Resistivity variation of Anisotropic magnetoresistance
$\Delta\rho$	Resistivity variation
$\Delta R$	Resistance variation
$\rho_{\text{tot}}$	Total resistivity
$\sigma$	Conductivity
$\Lambda_s$	Interface spin-scattering length

$\lambda_l$	Mean free path
$\gamma$	Secondary electron emission coefficient
$\omega$	angular velocity
AMR	Anisotropic magnetoresistance
AP	Antiparallel
AF	Antiferromagnetic
at%	Atomic percent
B	Magnetic induction
CIP	Current in Plane
CPP	Current Perpendicular to the Plane
CMR	Colossal Magnetoresistance
CVD	Chemical Vapor Deposition
$c_1$	Mean velocity of sputtered atoms
$d$	Lattice spacing
$\Delta d$	Variation in lattice spacing
$d_{\text{bulk}}$	Bulk lattice spacing
DC	Direct current
d.t.	Deposited temperature
e	Electron
EDX	Energy dispersive X-ray
E	Electric field
F	Ferromagnetism
GMR	Giant Magnetoresistance
H	Magnetic field
HBT	High electron mobility transistor

HEMET	Hetrojunction bipolar transistor
$H_{\max}$	maximum field
$H_s$	Saturation field
$I$	Current
$j$	Current density
$k$	Boltzman's constant
K	Kelvin
keV	Kilo-electron volt
kV	Kilo volt
L	Electrode spacing
LSI	Large Scale Integration
$L_{SF}$	Spin-diffusion length
m	Mass
M	Magnetisation
MBE	Molecular beam epitaxy
MESFET	Metal-semiconductor field effect transistor
MHz	Megahertz
$M_s$	Saturation magnetization
MOCVD	Metalorganic chemical vapour deposition
MR	Magnetoresistance
MRAM	magnetic RAM
$n_2$	Density of the discharge gas molecules
OMR	Ordinary magnetoresistance
Oe	oersted
P	pressure